

CIPM Key Comparison for Low-Pressure Gas Flow: CCM.FF-K6 Final Report

John Wright, Bodo Mikan, Richard Paton, Kyung-Am Park, Shin-ichi Nakao, Khaled Chahine, Roberto Arias

October 9, 2007

Introduction and Executive Summary

A key comparison between seven national metrology institutes in the area of low-pressure gas flow was organized by the Comité International des Poids et Mesures (CIPM) and the Working Group for Fluid Flow. The purpose of the comparison is to verify Calibration and Measurement Capabilities by 1) determining key comparison reference values (KCRVs), 2) calculating the difference between each participant's results and the KCRV, and 3) calculating the degrees of equivalence between the participants, all with uncertainty estimates (the "KC outputs"). The participants, the types of primary standards used, and the uncertainty of the facilities are listed in table 1. Uncertainties given in this report are standard ($k = 1$) values unless otherwise noted.

Table 1. Schedule and facilities used during the KC

Participant	Date	Type of primary standard	Standard uncertainty (%)
NIST (United States)	Mar 2005	34 L and 677 L PVT_t	0.025
PTB (Germany)	May 2005	Piston provers	0.075
		CFV working standards	0.04
		Positive displacement working standard	0.059 to 0.076
NEL (United Kingdom)	June 2005	Piston provers	0.08
NIST	July 2005	34 L and 677 L PVT_t	0.025
KRISS (Korea)	Aug 2005	12 L piston prover	0.065
		150 L and 600 L bell provers	0.055
NMIJ (Japan)	Oct 2005	Gravimetric	0.05
		PVT_t	0.075 to 0.1
NMIA (Australia)	Jan 2006	Piston provers	0.05
		Bell prover	0.08
NIST	Feb 2006	34 L and 677 L PVT_t	0.025
CENAM (Mexico)	April 2006	Piston provers	0.045
		Bell prover	0.075
NIST	May 2006	34 L and 677 L PVT_t	0.025

A set of 8 critical flow venturis with dedicated, redundant pressure and temperature sensors was the transfer standard (TS). The TS was used at seven mass flows of dry air: 4.4 g/min, 5 g/min, 5.6 g/min, 90 g/min, 130 g/min, 180 g/min, and 260 g/min. The two distinct flow ranges of the comparison were selected so that the participants could use two different primary standards and give a broader view of lab capabilities. All

participants submitted measurements at the three lowest flows, but due to pressure or flow range limitations, only two labs calibrated at all four Large TS flows. This meant that only four participant data sets were involved in calculating the KCRV at 260 g/min.

The KCRVs for each flow set point (and the other KC outputs) were calculated using the uncertainty weighted mean or median following the approach of Cox.¹ The degree of equivalence (difference from the KCRV) for each participant at each flow is shown in figure 1.

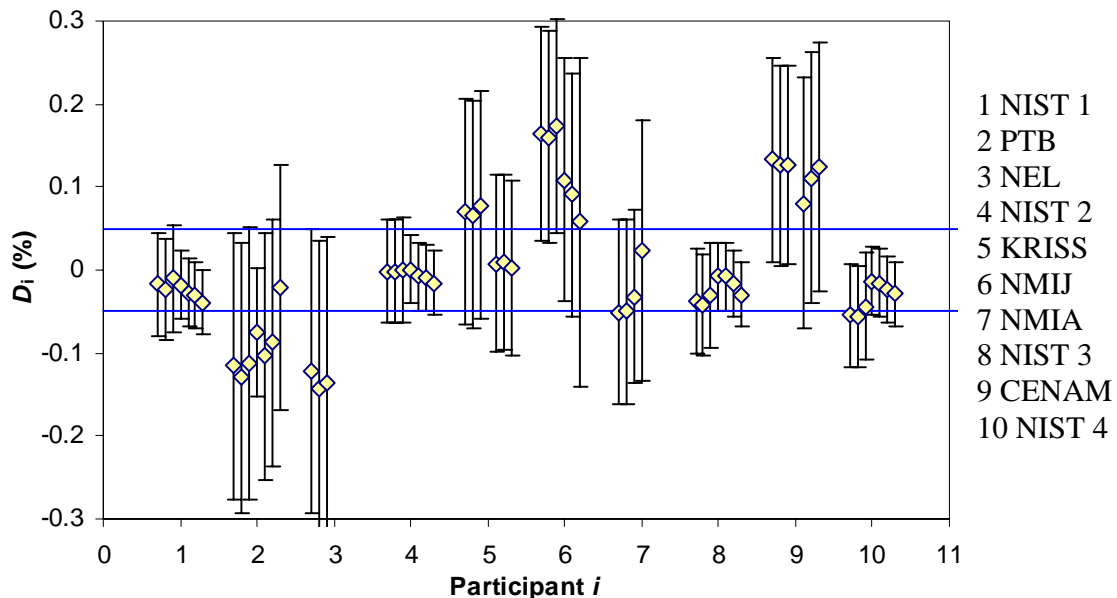


Figure 1. Degrees of equivalence. Each participant’s results are clustered in groups of up to 7 points (flow increasing from left to right). Horizontal lines represent the $k = 2$ uncertainty of the KCRV (0.05 %). Error bars are the $k = 2$ uncertainty in the degree of equivalence $U(D_i)$ of each lab to the KCRV.

Four calibration data sets collected at NIST are plotted in figure 1 to illustrate the stability of the TS during the comparison. Standard uncertainty due to calibration changes in the TS is less than 0.02 %. (Only the second NIST data set was used during KCRV calculations and in later presentations of KC results.) The drift observed in the TS calibrations at NIST is in accordance with values from a propagation of uncertainty analysis for the TS, 0.026 % and 0.019 % ($k = 1$) for the Small TS and Large TS respectively.

The Transfer Standard

The transfer standard (TS) is a set of eight critical flow venturis (CFVs) with dedicated pressure and temperature instrumentation. Most participants were able to test the TS with two CFVs in series. There are redundant sensors for measuring the CFV pressures and temperatures (2 upstream CFV pressures and temperatures, 2 downstream pressures and temperatures). The redundant pressure, temperature, and flow measurements allowed us to assess the TS calibration stability throughout the KC. Two additional temperature

¹ Cox, M. G., *The Evaluation of Key Comparison Data*, Metrologia, 2002, **39**, 589-595.

sensors measured the room and inlet gas temperature in order to assess the magnitude of temperature effects on the TS.

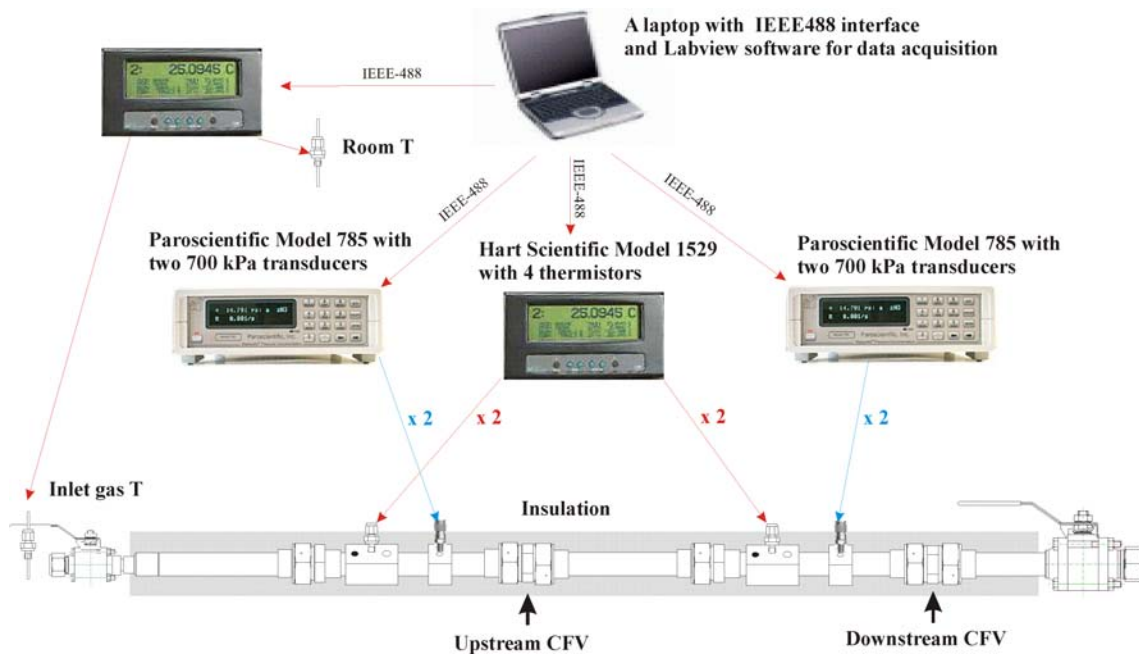


Figure 2. A schematic of the transfer standard.²

The 8 CFV's are normally tested as 4 pairs called Small A, Small B, Large A, and Large B (see figure 3). The pairs called Small A and Small B are nominally the same and are tested on different occasions. The same is true for the pairs called Large A and Large B. A lab that is able to perform all of the measurements in the test sequence makes 140 individual flow measurements (2 CFV sets × 7 flow set points × 5 repeats × 2 occasions). Some labs could not test two CFVs in series due to pressure limitations of their facilities. In these cases, the downstream CFVs were tested alone.³

K6 compared *mass flow* measurements from each lab using the discharge coefficient, C_d , for the eight CFVs:

$$C_d = \frac{\dot{m} \sqrt{(R/M) T_0}}{(\pi d^2/4) C_{*1} P_0} , \quad (1)$$

² Certain commercial equipment, instruments, or materials are identified in this paper to foster understanding. Such identification does not imply recommendation or endorsement, nor does it imply that the materials or equipment identified are necessarily the best available for the purpose.

³ Wright, J. D. and Kline, G. M., *Protocol for the CIPM Low-Pressure Gas Flow Key Comparison (CCM.FF-K6)*, NIST Fluid Metrology Group, July 27, 2005.

where \dot{m} is the mass flow from the participant, R is the universal gas constant, T_0 is the stagnation temperature, M is the molecular weight of the air, P_0 is the stagnation pressure, d is the diameter of the CFV throat, and C_{*i} is the critical flow function, a property of the gas calculated from its specific heat ratio. The molecular weight was calculated from the dew point temperature reported by the participants and dry air composition was used to calculate C_{*i} (see Appendix A). A C_d value was calculated for each CFV for each flow at which it was used.

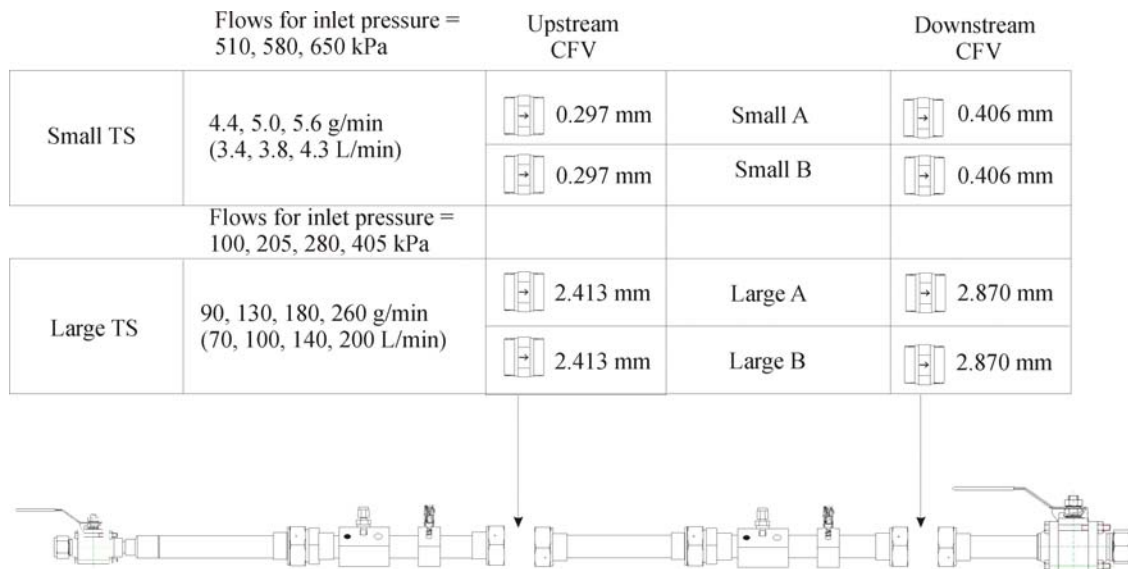


Figure 3. The TS uses two CFVs in series, switched, over two flow ranges.

Uncertainty Analysis

The uncertainty of the discharge coefficient used to compare the participants is due to 1) the uncertainty of the mass flow measurement, 2) the standard deviation of the mean of repeated measurements in each lab, and 3) uncertainties related to the transfer standard (drift, environmental sensitivities, etc). The root-sum-square of these components was used as $Cox's^1 u(x_i)$ during calculation of the uncertainty of the KCRV and the uncertainty of the degree of equivalence. The uncertainty of the TS was evaluated by propagation of uncertainties. This value was assessed by 1) comparison of four calibrations performed at NIST during the course of the KC, and 2) comparison of redundant flow measurements made at each lab.

Propagation of Uncertainties

We analyzed equation 1 following the method of propagation of uncertainties.^{4,5} This involves obtaining sensitivity coefficients by partial differentiation,

⁴ *Guide to the Expression of Uncertainty in Measurement*, International Organization for Standardization, Switzerland, 1993.

⁵ Coleman H W and Steele W G, *Experimentation and Uncertainty Analysis for Engineers*, 2nd ed., New York, John Wiley and Sons, 1999.

$S_i = (x_i/C_d)(\partial C_d/\partial x_i)$. We also obtained standard uncertainties $u(x_i)$ for the inputs to equation 1 from experiments with the instruments we used during the KC. The uncertainty components considered and their contribution to the uncertainty of the measurand are listed in tables 2 and 3 as a percentage of C_d . The sources and magnitudes of uncertainty components are explained in the comments below.

Table 2. Uncertainty contributions to the measurand (in percent of C_d) for the large CFVs.

Large CFVs		PTB	NEL	NIST	KRISS	NMIJ	NMIA	CENAM
1	Mass flow	0.04 to 0.076		0.025	0.055	0.075 to 0.10	0.08	0.075
2	Reproducibility	0.008		0.003	0.002	0.004	0.006	0.016
3	Pressure	0.013		0.013	0.013	0.013	0.013	0.013
4	Temperature (1/2)	0.002		0.002	0.002	0.002	0.002	0.002
5	Critical flow function	0.008		0.008	0.008	0.008	0.008	0.008
6	Molecular weight (1/2)	0.006		0.006	0.006	0.006	0.006	0.006
7	T effects	0.006		0.006	0.006	0.006	0.006	0.006
8	Critical flow effects	0.006		0.006	0.006	0.006	0.006	0.006
9	Leak	0		0	0	0	0	0
	Combined [$u(x_i)$, $k = 1$]	0.045 to 0.078		0.031	0.058	0.077 to 0.102	0.082	0.079
	Expanded ($k = 2$)	0.090 to 0.155		0.063	0.116	0.155 to 0.204	0.165	0.158

Table 3. Uncertainty contributions to the measurand (in percent of C_d) for the Small CFVs.

Small CFVs		PTB	NEL	NIST	KRISS	NMIJ	NMIA	CENAM
1	Mass flow	0.075	0.08	0.025	0.065	0.05	0.05	0.045
2	Reproducibility	0.005	0.012	0.001	0.002	0.002	0.004	0.004
3	Pressure	0.013	0.013	0.013	0.013	0.013	0.013	0.013
4	Temperature (1/2)	0.002	0.002	0.002	0.002	0.002	0.002	0.002
5	Critical flow function	0.008	0.008	0.008	0.008	0.008	0.008	0.008
6	Molecular weight (1/2)	0.006	0.006	0.006	0.006	0.006	0.006	0.006
7	T effects	0.016	0.016	0.016	0.016	0.016	0.016	0.016
8	Critical flow effects	0.006	0.006	0.006	0.006	0.006	0.006	0.006
9	Leak	0.010	0.010	0.010	0.010	0.010	0.010	0.010
	Combined [$u(x_i)$, $k = 1$]	0.079	0.085	0.036	0.070	0.056	0.056	0.052
	Expanded ($k = 2$)	0.159	0.170	0.072	0.140	0.113	0.113	0.104

1 Mass Flow: Each lab provided documentation of the uncertainty of their mass flow measurements. The pilot lab reviewed these documents, considered them credible, and they are listed in table 1. The K6 protocol asked that the uncertainties submitted by each lab be for the mass flow measurement alone, i.e. not including reproducibility or TS

uncertainties. Hence the values listed in tables 2 and 3 may not equal those found in the Calibration and Measurement Capabilities. For some labs, the reported mass flow uncertainty varied with the test conditions and they are shown in the tables as a range. Each lab also submitted traceability statements and we found that there are no traceability dependencies between the participants.

2 Reproducibility: The standard deviation of the mean of 40 normalized C_d values ($\langle C_d \rangle$, see equation 2) at each flow set point was used for the reproducibility in each lab (4 CFVs \times 10 measurements).

3 Pressure: All participants used the same pressure sensors at nominally the same pressures, so any biases in the pressure sensor calibrations are correlated and cancel. The sensors drifted in calibration during the comparison (up to 0.05 %) and they were subject to errors due to environmental temperature sensitivity. We examined 1) experimental data on the sensitivity of the pressure sensors to room temperature changes, 2) nine pressure sensor calibrations versus a piston pressure gage conducted on the four occasions that the TS was at NIST during the KC, and 3) the differences between redundant measurements made in each participant's lab (see Appendix B), and arrived at a standard uncertainty of 0.013 %.

4 Temperature: All participants used the same temperature sensors throughout the KC and calibration biases are correlated. Calibrations performed at NIST during the comparison showed the four CFV temperature sensors to be stable within 1 mK. The temperature measurement uncertainty in tables 2 and 3 also incorporates analysis of the redundant measurements shown in Appendix B. Since temperature appears under the square root in equation 1, its normalized sensitivity coefficient is 0.5.

5 Critical Flow Function: Errors in the value of C_{*i} are also highly correlated for measurements between different participants. The same correlation was used at nominally the same pressures and temperatures. The C_{*i} correlation we used assumes ideal gas behavior and dry air composition (see Appendix A). We have also run sample calculations of the real critical flow function, C_{*R} . To calculate C_{*R} we used thermodynamic functions from the NIST property database called Refprop.⁶ We integrated the entropy and enthalpy from the upstream conditions to the CFV throat conditions until the entropy at the endpoints was equal and the enthalpy change was equal to half of the sonic velocity at the throat squared. We examined two cases within the KC parameter space where the differences between C_{*i} and C_{*R} are the most extreme: 1) the case with the highest water content ($T_{dp} = 280$ K, $x_{H_2O} = 0.01$) and the 2) the highest pressure (645 kPa). We found that the differences between the real and ideal critical flow function values were less than 0.012 %. Applying a rectangular distribution to this difference results in a standard uncertainty of $0.012 \% / \sqrt{3} = 0.008 \%$ for C_{*i} . We used C_{*i} instead of C_{*R} because of software complications in calculating C_{*R} and because the uncertainties due to using C_{*i} are acceptably small.

⁶ Lemmon, E., McLinden, M., and Huber, M., 2002, *Refprop 23: Reference Fluid Thermodynamic and Transport Properties*, NIST Standard Reference Database 23, Version 7.0, 7/30/02, National Institute of Standards and Technology, Boulder, Colorado.

6 Molecular Weight: Participants were asked to report both the molecular weight and the dew point temperature (T_{dp}) of the air used for the KC. We calculated the molecular weight from the dew point temperature by the algorithm described in Appendix A. We found that for all but two of the labs, the reported values of M and those calculated from T_{dp} agreed within 0.019 %. After conferring with these two labs, we based our values of M on the dew point temperature. We will use a standard uncertainty for the molecular weight of 0.019 % / $\sqrt{3}$ = 0.011 % and it has a normalized sensitivity of 0.5 due to the square root function in equation 1. The uncertainties of the molecular weight of dry air (0.0035 %) and of water are negligible compared to 0.011 %.

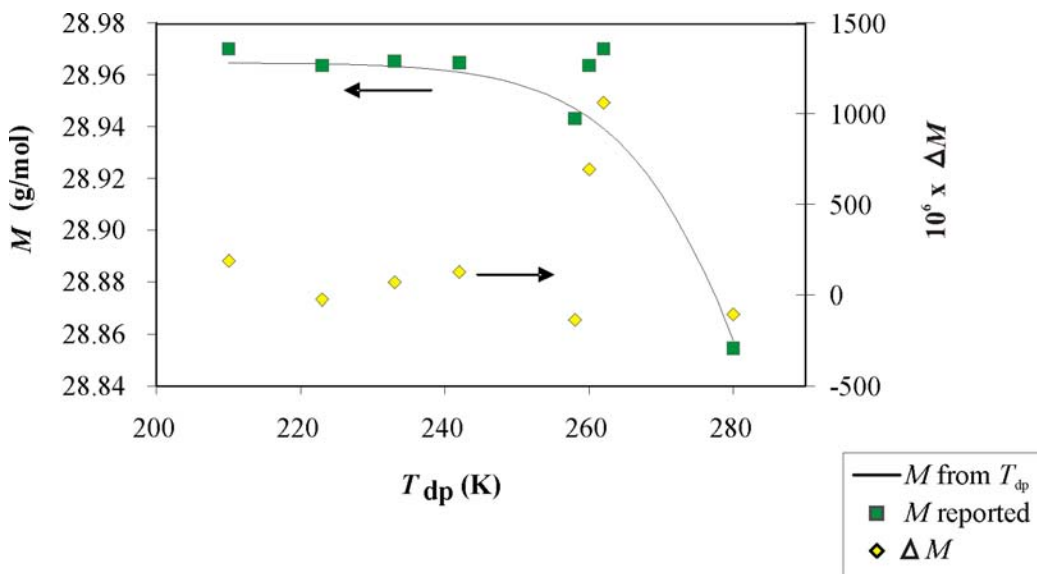


Figure 4. Molecular weight of the air used in the KC, reported and calculated from the reported dew point temperature.

7 Temperature Effects: The CFVs in the transfer standard are influenced by the temperature of the metered gas and the room temperature via 1) thermal expansion of the CFV throat area, 2) thermal boundary layer effects on mass flux at the throat, 3) temperature differences between the sensor location and the CFV entrance caused by heat transfer from the room to the metered gas. The uncertainty caused by these effects was evaluated in studies at the pilot lab⁷ and controlled during the course of the comparison by insulating the TS and placing limits on the temperature conditions: room temperature between 19 °C and 27 °C and $|T_{gas} - T_{room}| < 3$ °C. The actual range of room temperature conditions during the course of the comparison was 19.5 °C to 25.8 °C. The maximum difference between the room and CFV gas temperature was 1.6 K. Based on these temperature conditions and the preliminary temperature studies on the TS, the standard uncertainty due to temperature effects is 0.016 % for the small CFVs and 0.006 % for the large CFVs.

⁷ Wright, J. D., *Uncertainty of the Critical Venturi Transfer Standard Used in the K6 Gas Flow Key Comparison*, Proceedings of Flomeko 2007, Johannesburg, South Africa, in review.

8 *Critical Flow Effects*: Preliminary tests of the TS showed that the small downstream nozzles are not truly critical even for the pressure ratio of $P_{up} / P_{down} = 235 \text{ kPa} / 107 \text{ kPa} = 2.2$ or greater recommended in the protocol. The standard uncertainty due to lack of perfect criticality under the permitted outlet pressure conditions is 0.006 %.⁷

9 *Leaks*: A leak checking procedure was used each time the TS piping was rearranged. A program calculated the leak flow based on the rate of change of the gas density in the TS while it was pressurized and the inlet and outlet valves were closed. The leaks were controlled to less than 0.01 % of the minimum flow of the comparison. This leak is negligible for the Large TS.

Uncertainties related to the universal gas constant and the CFV throat diameter can be ignored since the same values were used throughout the C_d calculations and they are completely correlated. Taking the root-sum-square of the components related to the TS (components 3 through 9 in tables 2 and 3) gives standard uncertainties of 0.026 % and 0.019 % for the Small and Large TS respectively. The larger uncertainty for the Small TS is due to temperature effects and leaks.

Agreement of Four Flow Calibrations at NIST

The TS was calibrated with the NIST 34 L and 677 L *PVTt* standards on four occasions during the KC. The change in calibration with respect to the first calibration is plotted for the Small and Large TS in figures 5 and 6 respectively. All four NIST calibrations are also shown in figure 1. The second NIST calibration (July 2005) was used as the NIST entry in the KC.

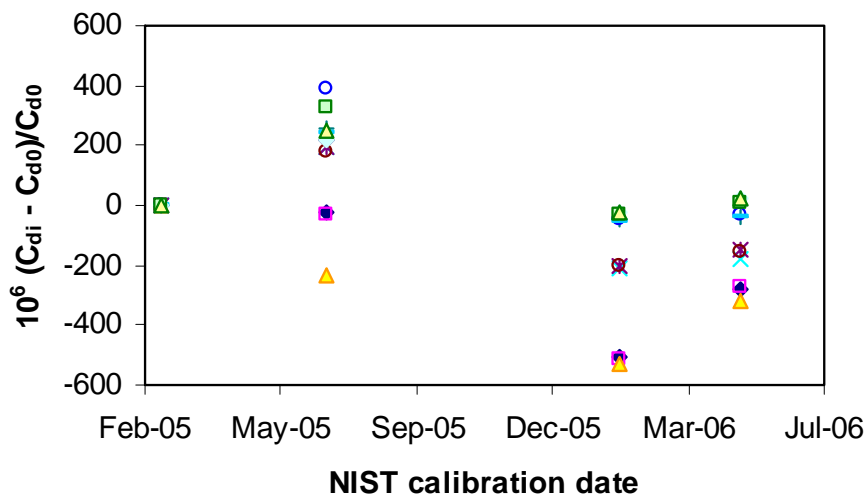


Figure 5. Change in small CFV calibrations during the KC based on four calibrations at NIST. Data for four nozzles at three flows shown, standard deviation = 0.02 %

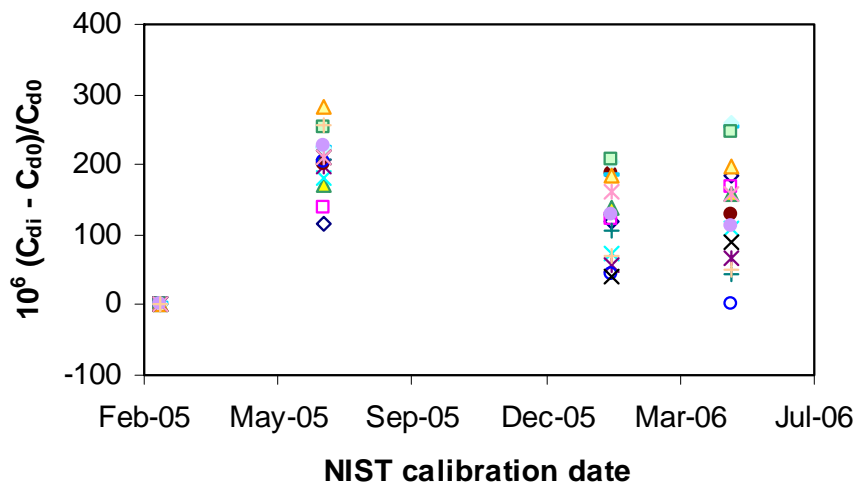


Figure 6. Change in large CFV calibrations during the KC based on four calibrations at NIST. Data for four nozzles at four flows shown, standard deviation = 0.009 %.

Uncertainties due to M , C_{*i} , and temperature effects will be highly correlated between the four NIST calibrations. Hence we expect to see smaller changes between the NIST calibrations than the uncertainties we calculated by propagation of uncertainty, and that is the case.

Agreement of Redundant Flow Measurements in Participating Labs

When $C_{d,KCRV}$ values are used to calculate flows from the TS, the differences in upstream and downstream flows measured with the CFVs have standard deviations of 0.017 % for the small CFVs and 0.009 % for the large CFVs, within our expectations based on the propagation of uncertainties analysis.

In summary, the four calibrations performed in the pilot lab during the comparison and the agreement of the redundant flow measurements by the TS within each participant's lab confirm a TS uncertainty of 0.026 % or less during the entire comparison. We consider the values from the propagation of uncertainty analysis (tables 2 and 3) confirmed and we will use them during calculation of the KC outputs.

Data Processing and Calculation of the KC Outputs

The KC outputs were calculated following the procedures recommended by Cox.¹ First, uncertainty weighted mean values for C_d were calculated. The chi-squared consistency check failed for all of the flow set points for the Small TS, leading us to calculate the median and perform Monte Carlo simulations to obtain the KC outputs for the three smallest comparison flows. For these three flows, we also investigated the uncertainty weighted mean after removal of discrepant results, using the chi-squared statistic at the 5 % level of significance as the criterion for removal. We found that the procedure that removed discrepant results led to discontinuities in the KCRV as a function of flow due to the exclusion of different labs at different flow set points. After review of the three methods (all plotted in Appendix C), we used the KCRV based on the median to calculate

the Small TS KC outputs. The largest difference between KCRV values calculated by the three methods was 0.053 % and generally the median fell between the two other alternatives.

For the Large TS, all but one CFV at one flow passed the chi-squared consistency check and it was decided for simplicity of data processing to use the uncertainty weighted result as the KCRV for all of the Large TS flows. The KCRV based on the uncertainty weighting and the median are plotted in Appendix C and the largest difference between the two procedures was 0.038 %, but for most flows it was less than 0.01 %.

Errors in achieving the same flow conditions in each lab were minimized by aligning C_d values so that they were all for the same $Re^{-0.5}$ values. The values of the slopes $dC_d/d(Re^{-0.5})$ used for the adjustments were based on the individual participant's data, except in the few cases where a lab used a CFV at only one flow. In these cases, a slope based on all participants' data was used.

The median or uncertainty weighted mean of individual C_d measurements from all the participants was calculated and used as $C_{d\text{KCRV}}$ except for the case of the 90 g/min data for the large, upstream CFVs. Limitations on the operating conditions of the participant's primary standards prevented all but two labs (NIST and NMIJ) from testing the large upstream CFVs at 90 g/min. Data from all labs at all flows were used to obtain a first-order, linear regression of the median C_d as a function of $Re^{-0.5}$ and this was used to calculate $C_{d\text{KCRV}}$ for the large upstream CFVs at 90 g/min.

The ten C_d values from each participant for each CFV at each flow were averaged to obtain \bar{C}_d . The participants' \bar{C}_d values were normalized by the KCRV:

$$\langle \bar{C}_d \rangle = \frac{\bar{C}_d}{C_{d\text{KCRV}}} = \frac{\dot{m}}{\dot{m}_{\text{KCRV}}}, \quad (2)$$

so that data for the same flow measured with different CFVs could be averaged. This normalized C_d is equivalent to the ratio of the mass flow measured by a particular participant to the mass flow based on the results of all of the participants. The normalized KCRV, $\langle C_{d\text{KCRV}} \rangle$, has the value 1.

In most cases, four CFVs were used at each flow set point. The results from multiple nozzles used at the same flow were averaged to obtain $\langle \bar{C}_d \rangle$, the ratio of each participants results to the KCRV, normally based on 40 individual flow measurements made with four CFVs (in a few cases 20 measurements from two CFVs). This is the quantity that is given in the subsequent displays of data. The standard deviation of the mean of the 40 measurements was used as the reproducibility and is listed for each lab in tables 2 and 3.

In the following tables of results we will use the nomenclature of Cox, where x_i is participant i 's result $\langle \bar{C}_d \rangle$ at a particular flow, D_i is the degree of equivalence for

participant i (difference between x_i and the KCRV), $U(D_i)$ is the approximate 95 % confidence level ($k = 2$) uncertainty for D_i , $D_{i,j}$ is the degree of equivalence between participants i and j ($D_{i,j} = x_i - x_j$), and $U(D_{i,j})$ is the 95 % confidence level ($k = 2$) uncertainty for $D_{i,j}$.

Comparison Results

Tables 4 and 5 show the degrees of equivalence for the flows covered by the Small TS and Large TS respectively.

Table 4. Results for the Small TS at 4.4 g/min, 5 g/min, and 5.6 g/min.

Small TS	4.4 g/min		5.0 g/min		5.6 g/min	
	D_i	$U(D_i)$				
	(%)					
PTB	-0.121	0.161	-0.133	0.163	-0.123	0.164
NEL	-0.128	0.171	-0.145	0.177	-0.146	0.176
NIST	-0.006	0.063	-0.004	0.061	-0.010	0.064
KRISS	0.064	0.136	0.064	0.136	0.067	0.137
NMIJ	0.160	0.129	0.157	0.128	0.163	0.129
NMIA	-0.055	0.112	-0.054	0.111	-0.042	0.105
CENAM	0.128	0.123	0.122	0.121	0.117	0.120

Table 5. Results for the Large TS at 90 g/min, 130 g/min, 180 g/min, and 260 g/min.

Large TS	90 g/min		130 g/min		180 g/min		260 g/min	
	D_i	$U(D_i)$						
	(%)							
PTB	-0.076	0.077	-0.104	0.149	-0.087	0.149	-0.021	0.148
NEL								
NIST	0.001	0.041	-0.008	0.041	-0.009	0.040	-0.016	0.038
KRISS			0.008	0.106	0.010	0.106	0.002	0.105
NMIJ	0.109	0.147	0.090	0.147	0.058	0.198		
NMIA	0.024	0.157						
CENAM			0.081	0.151	0.111	0.151	0.125	0.150

Figures 7 and 8 present the KC results for the Small TS and Large TS respectively.

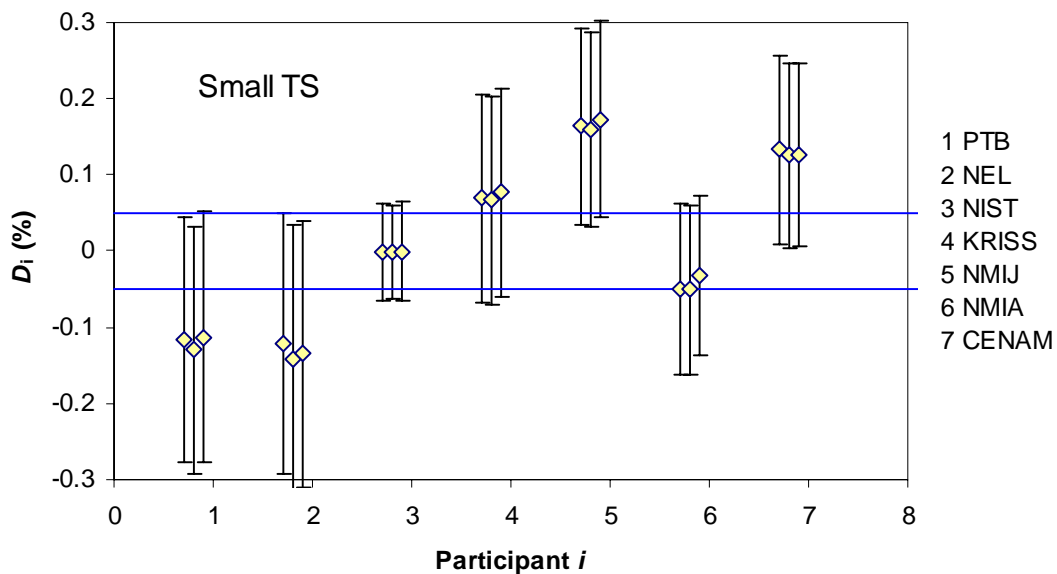


Figure 7. Degrees of equivalence for the Small TS. Flows of 4.4 g/min, 5 g/min, and 5.6 g/min (left to right) are represented as individual points clustered for each participant. Horizontal lines represent the $k = 2$ uncertainty of the KCRV (0.05 %). Error bars are the $k = 2$ uncertainty in the degree of equivalence of each lab to the KCRV.

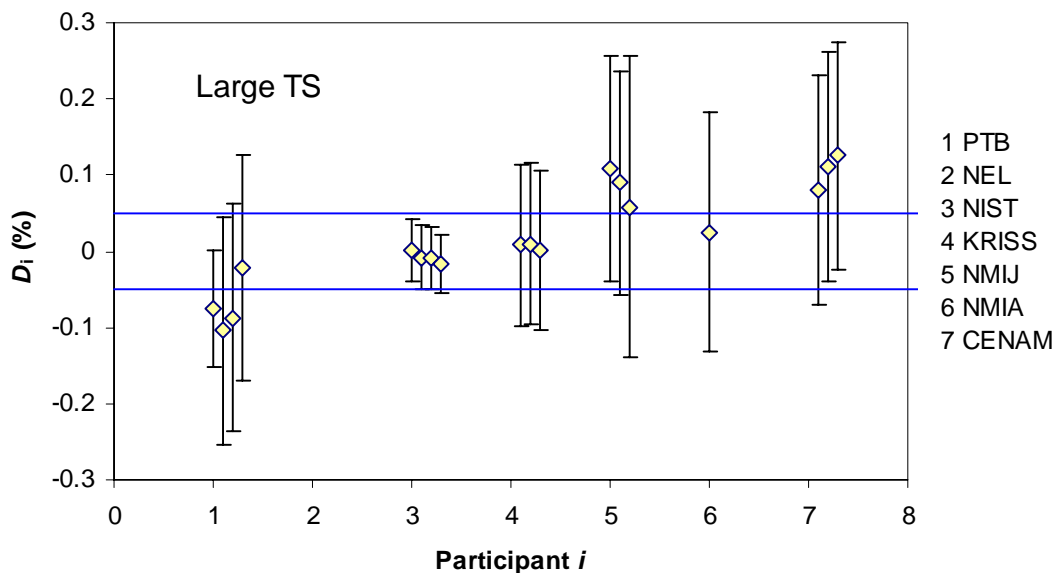


Figure 8. Degrees of equivalence for the Large TS. Flows of 90 g/min, 130 g/min, 180 g/min, and 260 g/min (left to right) are represented as individual points clustered for each participant. Horizontal lines represent the $k = 2$ uncertainty of the KCRV (0.05 %). Error bars are the $k = 2$ uncertainty in the degree of equivalence of each lab to the KCRV.

Tables 6 through 12 present the lab-to-lab degrees of equivalence for the 7 flows tested.

Table 6. Degrees of equivalence D_{ij} for 4.4 g/min. $D_{i,j} = x_i - x_j$, $U(D_{i,j})$ is a $k = 2$ value.

4.4 g/min	PTB		NEL	NIST	KRISS	NMIJ	NMIA	CENAM						
	$D_{i,j}$	$U(D_{i,j})$												
(%)														
PTB			0.005	0.234	-0.114	0.173	-0.184	0.213	-0.281	0.195	-0.064	0.193	-0.248	0.190
NEL	-0.005	0.234			-0.119	0.184	-0.189	0.222	-0.286	0.203	-0.069	0.203	-0.253	0.199
NIST	0.114	0.173	0.119	0.184			-0.070	0.158	-0.167	0.133	0.050	0.133	-0.134	0.126
KRISS	0.184	0.213	0.189	0.222	0.070	0.158			-0.097	0.181	0.120	0.178	-0.063	0.176
NMIJ	0.281	0.195	0.286	0.203	0.167	0.133	0.097	0.181			0.216	0.159	0.033	0.152
NMIA	0.064	0.193	0.069	0.203	-0.050	0.133	-0.120	0.178	-0.216	0.159			-0.184	0.153
CENAM	0.248	0.190	0.253	0.199	0.134	0.126	0.063	0.176	-0.033	0.152	0.184	0.153		

Table 7. Degrees of equivalence D_{ij} for 5 g/min.

5.0 g/min	PTB		NEL	NIST	KRISS	NMIJ	NMIA	CENAM						
	$D_{i,j}$	$U(D_{i,j})$												
(%)														
PTB			0.013	0.233	-0.127	0.174	-0.197	0.211	-0.291	0.195	-0.079	0.195	-0.254	0.189
NEL	-0.013	0.233			-0.140	0.185	-0.210	0.220	-0.304	0.203	-0.092	0.204	-0.267	0.199
NIST	0.127	0.174	0.140	0.185			-0.070	0.157	-0.163	0.134	0.049	0.134	-0.127	0.128
KRISS	0.197	0.211	0.210	0.220	0.070	0.157			-0.093	0.178	0.118	0.180	-0.057	0.174
NMIJ	0.291	0.195	0.304	0.203	0.163	0.134	0.093	0.178			0.212	0.159	0.036	0.155
NMIA	0.079	0.195	0.092	0.204	-0.049	0.134	-0.118	0.180	-0.212	0.159			-0.175	0.153
CENAM	0.254	0.189	0.267	0.199	0.127	0.128	0.057	0.174	-0.036	0.155	0.175	0.153		

Table 8. Degrees of equivalence D_{ij} for 5.6 g/min.

5.6 g/min	PTB		NEL	NIST	KRISS	NMIJ	NMIA	CENAM						
	$D_{i,j}$	$U(D_{i,j})$												
(%)														
PTB			0.023	0.234	-0.112	0.174	-0.190	0.210	-0.285	0.196	-0.080	0.195	-0.239	0.190
NEL	-0.023	0.234			-0.135	0.183	-0.213	0.219	-0.308	0.204	-0.103	0.204	-0.262	0.197
NIST	0.112	0.174	0.135	0.183			-0.078	0.156	-0.172	0.134	0.032	0.134	-0.126	0.126
KRISS	0.190	0.210	0.213	0.219	0.078	0.156			-0.094	0.178	0.109	0.180	-0.049	0.172
NMIJ	0.285	0.196	0.308	0.204	0.172	0.134	0.094	0.178			0.204	0.161	0.046	0.153
NMIA	0.080	0.195	0.103	0.204	-0.032	0.134	-0.109	0.180	-0.204	0.161			-0.158	0.155
CENAM	0.239	0.190	0.262	0.197	0.126	0.126	0.049	0.172	-0.046	0.153	0.158	0.155		

Table 9. Degrees of equivalence D_{ij} for 90 g/min.

90 g/min	PTB		NEL	NIST	KRISS	NMIJ	NMIA	CENAM						
	$D_{i,j}$	$U(D_{i,j})$												
(%)														
PTB				-0.077	0.109		-0.184	0.178	-0.100	0.187				
NEL														
NIST	-0.077	0.109					-0.108	0.166	-0.024	0.175				
KRISS														
NMIJ	0.184	0.178		0.108	0.166				0.084	0.225				
NMIA	0.100	0.187		0.024	0.175			-0.084	0.225					
CENAM														

Table 10. Degrees of equivalence D_{ij} for 130 g/min.

130 g/min	PTB		NEL	NIST	KRISS	NMIJ	NMIA	CENAM					
	D_{ij}	$U(D_{ij})$											
(%)													
PTB				-0.097	0.168	-0.112	0.194	-0.195	0.219			-0.185	0.222
NEL													
NIST	0.097	0.168				-0.016	0.132	-0.098	0.166			-0.088	0.170
KRISS	0.112	0.194		0.016	0.132			-0.082	0.193			-0.073	0.196
NMIJ	0.195	0.219		0.098	0.166	0.082	0.193					0.010	0.221
NMIA													
CENAM	0.185	0.222		0.088	0.17	0.073	0.196	-0.010	0.221				

Table 11. Degrees of equivalence D_{ij} for 180 g/min.

180 g/min	PTB		NEL	NIST	KRISS	NMIJ	NMIA	CENAM					
	D_{ij}	$U(D_{ij})$											
(%)													
PTB				-0.078	0.168	-0.097	0.194	-0.145	0.257			-0.198	0.222
NEL													
NIST	0.078	0.168				-0.019	0.132	-0.067	0.213			-0.120	0.170
KRISS	0.097	0.194		0.019	0.132			-0.048	0.235			-0.101	0.196
NMIJ	0.145	0.257		0.067	0.213	0.048	0.235					-0.053	0.258
NMIA													
CENAM	0.198	0.222		0.120	0.170	0.101	0.196	0.053	0.258				

Table 12. Degrees of equivalence D_{ij} for 260 g/min.

260 g/min	PTB		NEL	NIST	KRISS	NMIJ	NMIA	CENAM					
	D_{ij}	$U(D_{ij})$											
(%)													
PTB				-0.005	0.168	-0.023	0.194					-0.146	0.222
NEL													
NIST	0.005	0.168				-0.018	0.132					-0.141	0.170
KRISS	0.023	0.194		0.018	0.132							-0.124	0.196
NMIJ													
NMIA													
CENAM	0.146	0.222		0.141	0.170	0.124	0.196						

Appendix A: CFV Calculations

The calculations of CFV discharge coefficient generally follow the procedures and nomenclature of the ISO 9300:2005(E) standard.⁸

Calculation of C_d from Mass Flow

The four pressure measurements were corrected for linear calibration drift based on the number of days since an initial calibration performed on February 25, 2005. Averages of redundant measurements of pressure and temperature for each nozzle were used.

The molecular weight M of air was calculated from the dew point temperature T_{dp} provided by the participating labs. The mole fraction of water was calculated by:

$$x_{H_2O} = \frac{P_{ws}(T_{dp})}{101.325 \text{ kPa}} , \quad (A1)$$

where P_{ws} is the saturation water vapor pressure, calculated from T_{dp} via a best fit function.^{9,10}

The molecular weight of moist air was calculated using the formula:

$$M = (1 - x_{H_2O})M_{Air} + x_{H_2O}M_{H_2O} , \quad (A2)$$

where M_{Air} is the molecular weight of dry air¹¹ (28.964643 g/gmol) and M_{H_2O} is the molecular weight of water (18.015 g/gmol).

An approximate value for the specific heat ratio (γ_1) based on the measured pressure and temperature values (P_1 and T_1) was calculated using a fit to the Refprop database for dry air.^{11,12} The speed of sound was calculated via:

$$a = \sqrt{\gamma_1 RT_1 / M} , \quad (A3)$$

⁸ International Organization Standardization, *Measurement of Gas Flow by Means of Critical Flow Venturi Nozzles*, ISO 9300:2005(E) 2nd edition.

⁹ American Society of Heating, Refrigerating and Air-Conditioning Engineers, *1993 ASHRAE Handbook: Fundamentals*, Atlanta, Georgia, pp. 6.7.

¹⁰ Hyland, R. W. and Wexler, A., *Formulations for the Thermodynamic Properties of the Saturated Phases of H₂O from 173.25 K to 473.15 K*, ASHRAE Transactions 89(2A), pp. 500 to 519, 1983.

¹¹ Wright, J., *Gas Properties Equations for the NIST Fluid Flow Group Gas Flow Measurement Calibration Services*, 2/04.

¹² Lemmon, E., McLinden, M., and Huber, M., 2002, *Refprop 23: Reference Fluid Thermodynamic and Transport Properties*, NIST Standard Reference Database 23, Version 7.0, 7/30/02, National Institute of Standards and Technology, Boulder, Colorado.

where R is the universal gas constant, $8314.471(\text{m}^2 \text{ g})/(\text{s}^2 \text{ K gmol})$. The velocity of the gas in the approach tube was calculated via the continuity equation,

$$u = \frac{4\dot{m} R T_1 Z}{\pi D^2 P_1 M}, \quad (\text{A4})$$

Where \dot{m} is the mass flow reported by the participating lab, Z is the gas compressibility, and D is the inside diameter of the approach pipe (22.23 mm). The compressibility was evaluated at T_1 and P_1 using a Refprop fit.¹¹ The Mach number (Ma) in the approach piping is u/a . The Mach number and specific heat ratio were used to calculate the stagnation temperature and pressure,

$$P_0 = P_1 \left[1 + \frac{\gamma_1 - 1}{2} (\text{Ma})^2 \right]^{\frac{\gamma_1}{\gamma_1 - 1}}, \quad (\text{A5})$$

$$T_0 = T_1 \left[1 + \frac{\gamma_1 - 1}{2} (\text{Ma})^2 (1 - \alpha) \right], \quad (\text{A6})$$

Where α is the recovery factor for the temperature sensor (0.75). A new value for the specific heat ratio (γ_0) based on the stagnation pressure and temperature values was calculated using the Refprop best fit correlation. The specific heat ratio was used to obtain the ideal critical flow function:

$$C_{*i} = \sqrt{\gamma_0 \left(\frac{2}{\gamma_0 + 1} \right)^{\frac{\gamma_0 + 1}{\gamma_0 - 1}}}. \quad (\text{A7})$$

The theoretical CFV mass flow was,

$$\dot{m}_{\text{th}} = \frac{(\pi d^2 / 4) C_{*i} P_0}{\sqrt{(R/M) T_0}}, \quad (\text{A8})$$

where d is the CFV throat diameter. The viscosity for the stagnation conditions (μ_0) was calculated from P_0 and T_0 using a Refprop best fit¹¹ and the theoretical Reynolds number was calculated with,

$$\text{Re}_{\text{th}} = \frac{4 \dot{m}_{\text{th}}}{\pi d \mu_0}. \quad (\text{A9})$$

The discharge coefficient is:

$$C_d = \frac{\dot{m}}{\dot{m}_{th}} . \quad (A10)$$

Calculation of Mass Flow from the CFVs

The flows from the upstream and downstream CFVs were compared as a diagnostic tool and to assess the uncertainty contributed by the TS to the comparison. To calculate mass flow from the CFV, a different process was used to calculate the Mach number. First the critical pressure ratio was calculated,

$$r_* = \left(\frac{2}{\gamma + 1} \right)^{\frac{\gamma}{\gamma - 1}} , \quad (A11)$$

And then it was used to obtain the Mach number:

$$\text{Ma} = \frac{(r_*)^{\frac{1}{\gamma}} \left[\frac{2}{\gamma - 1} \left(1 - (r_*)^{\frac{\gamma - 1}{\gamma}} \right) \right]^{\frac{1}{2}}}{\left[\left(\frac{D}{d} \right)^4 - (r_*)^{\frac{2}{\gamma}} \right]^{\frac{1}{2}}} . \quad (A12)$$

The discharge coefficients used in the mass flow calculations were obtained from a linear regression of all the calibrations of the KC,

$$C_{d \text{ fit}} = a_0 + \frac{a_1}{\sqrt{\text{Re}_{th}}} , \quad (A13)$$

And the CFV mass flow equals,

$$\dot{m} = C_{d \text{ fit}} \dot{m}_{th} . \quad (A14)$$

Appendix B: Difference between Redundant P and T Sensors

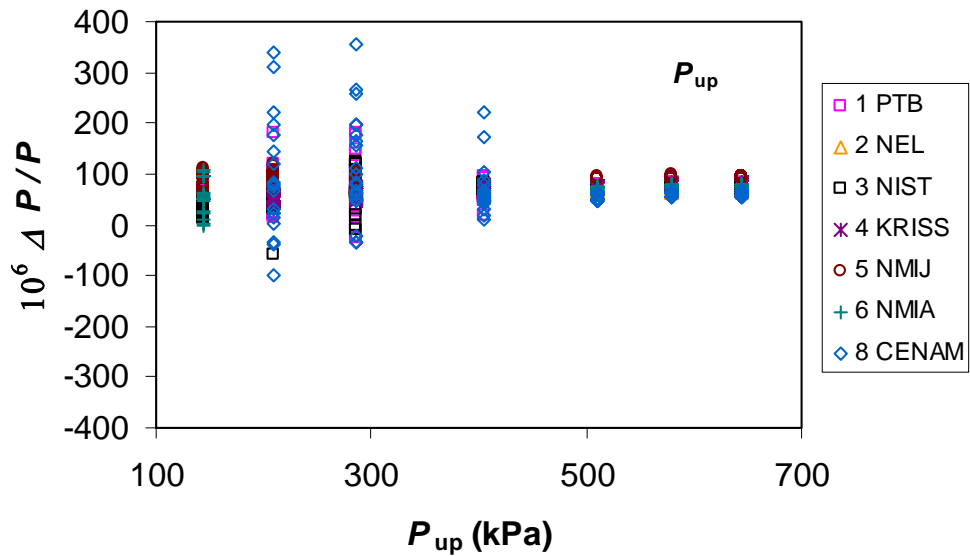


Figure B1. Differences for upstream CFV pressure measurements in each lab.

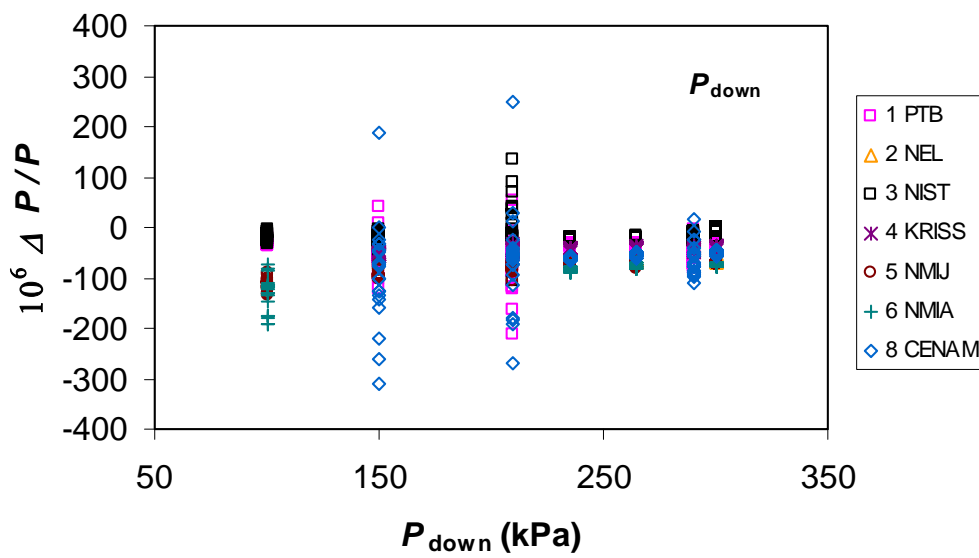


Figure B2. Differences for downstream CFV pressure measurements in each lab.

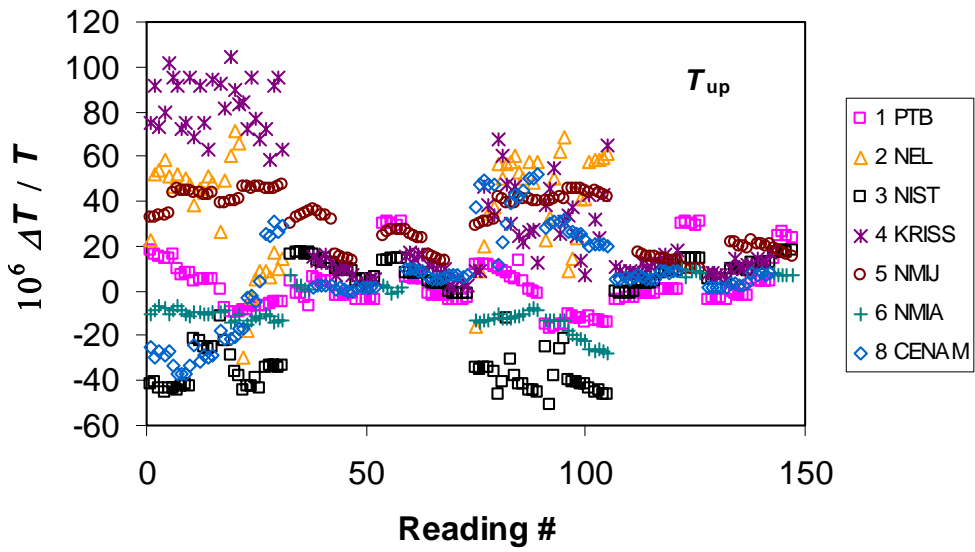


Figure B3. Differences for upstream CFV temperature measurements in each lab.

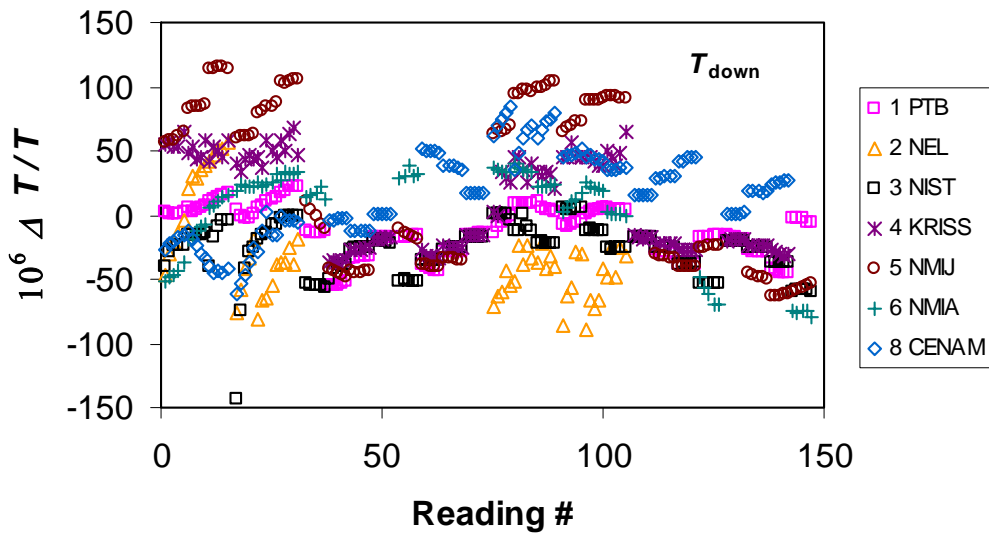


Figure B4. Differences for downstream CFV temperature measurements in each lab.

Appendix C: Graphical Display of Individual C_d Values and C_d KCRV

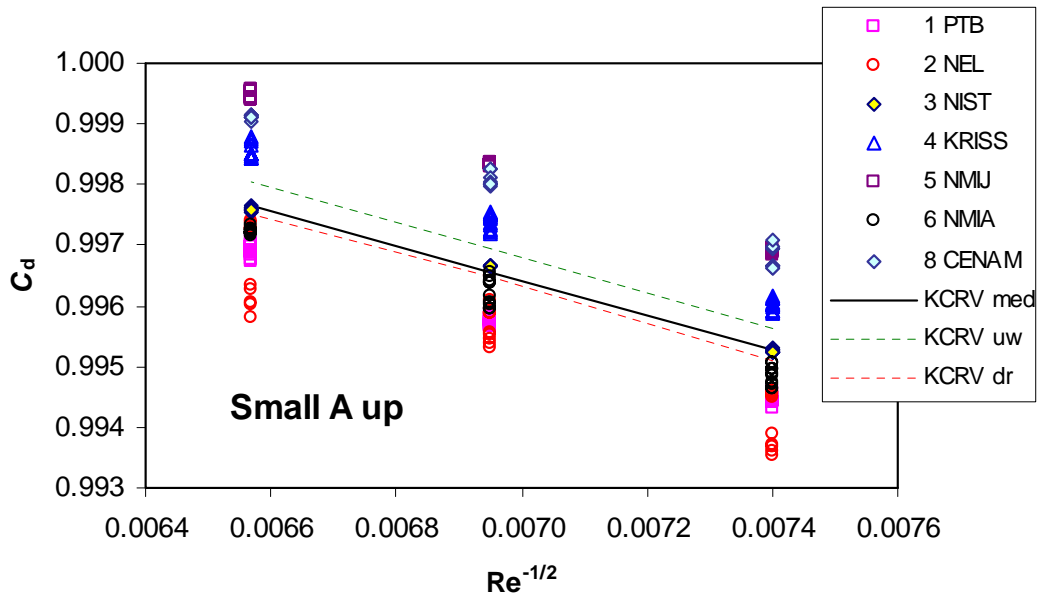


Figure C1. Results for CFV Small A Up. “KCRV med” represents the result from the median calculation, “KCRV uw” is the uncertainty weighted result, and “KCRV dr” is the uncertainty weighted result with discrepant values removed.

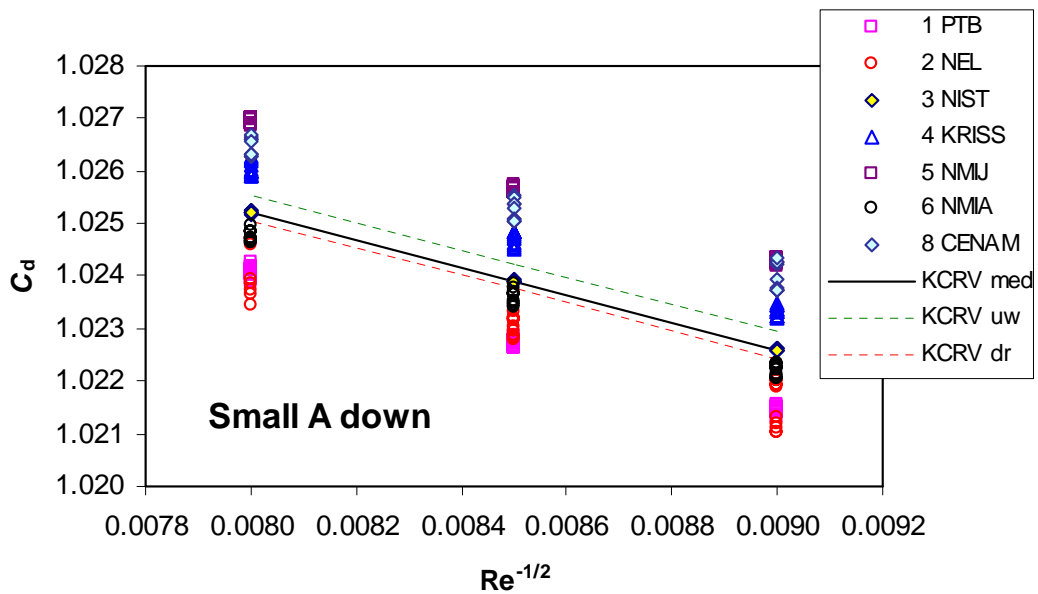


Figure C2. Results for CFV Small A Down

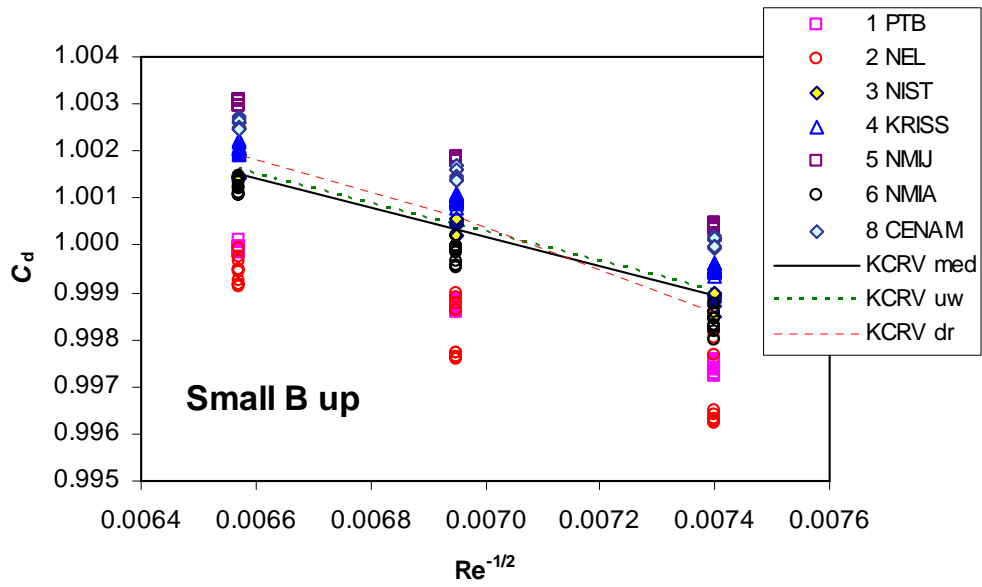


Figure C3. Results for CFV Small B Up

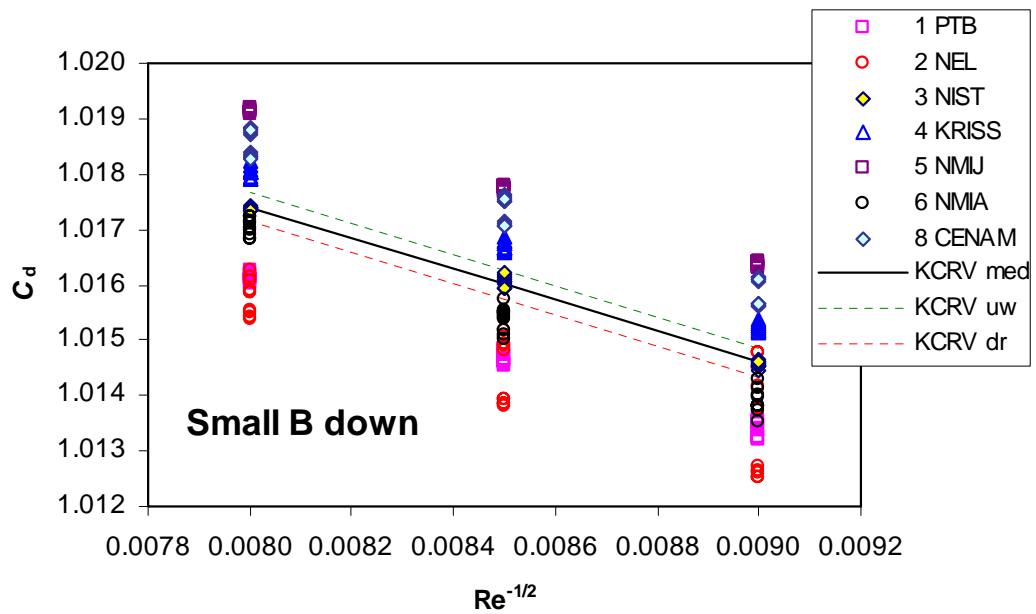


Figure C4. Results for CFV Small B Down

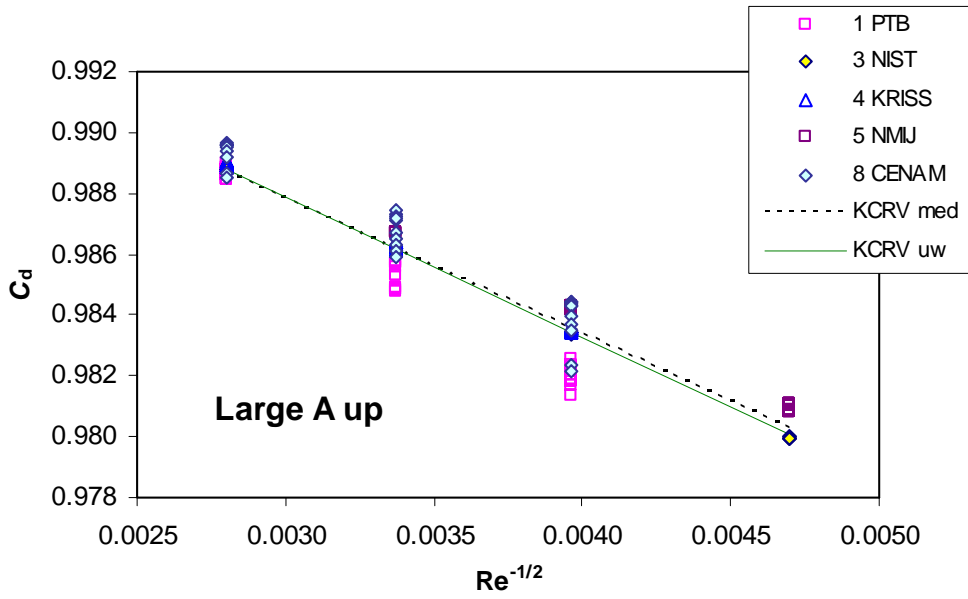


Figure C5. Results for CFV Large A Up

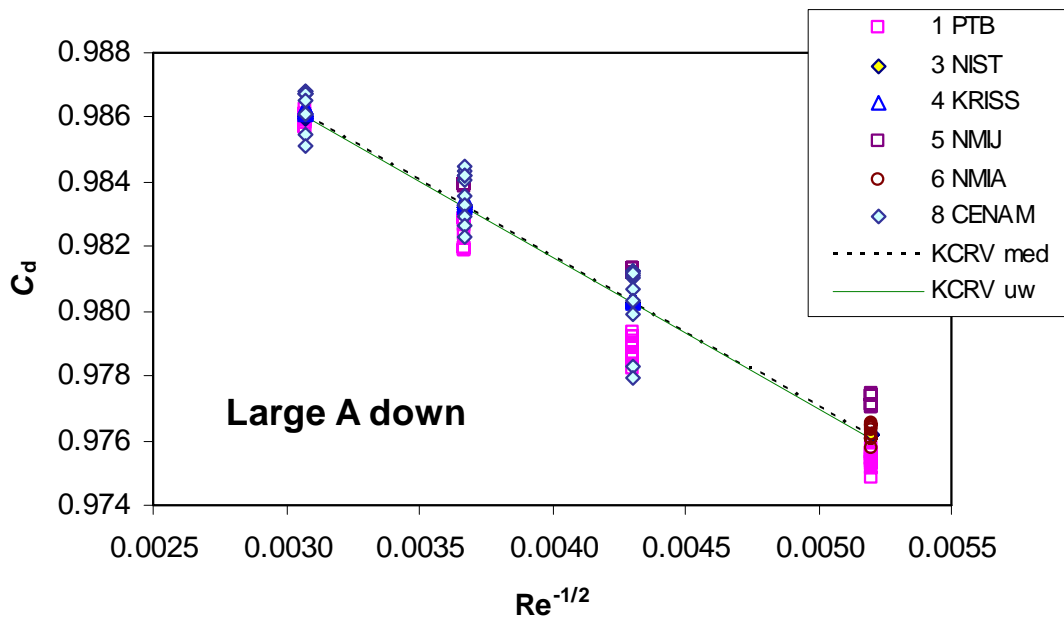


Figure C6. Results for CFV Large A Down

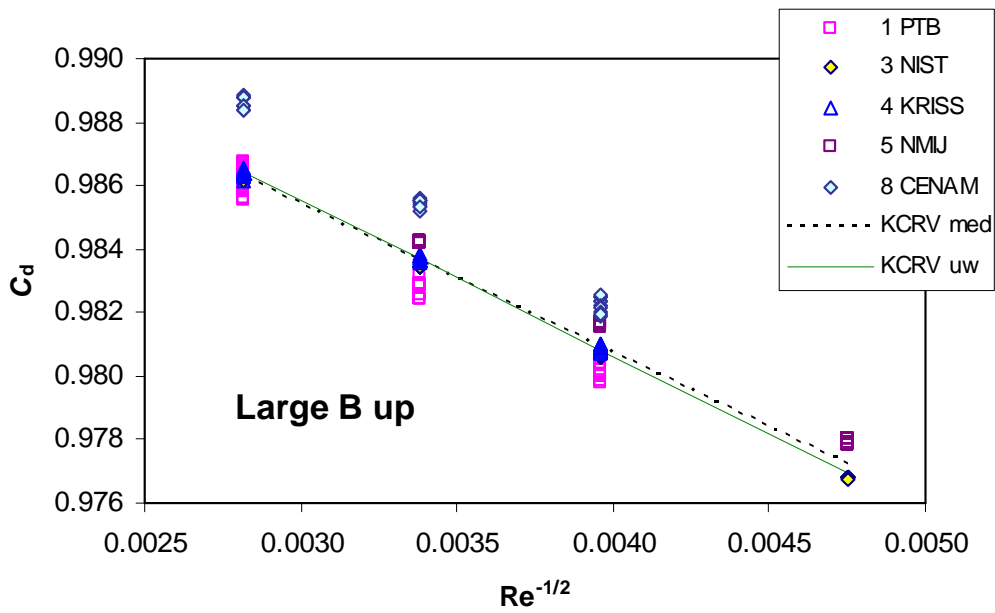


Figure C7. Results for CFV Large B Up

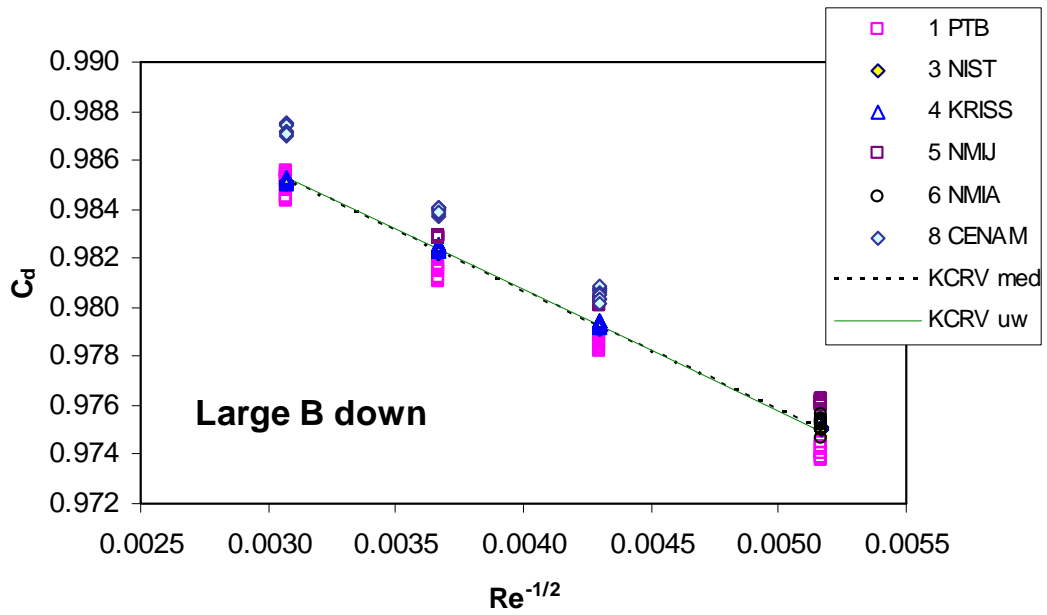


Figure C8. Results for CFV Large B Down